E. J. W. Van Someren et al. (Eds.)
Progress in Brain Research, Vol. 193
ISSN: 0079-6123

CHAPTER 21

Multimodal neuroimaging in patients with disorders of consciousness showing "functional hemispherectomy"

M. A. Bruno[†,1], D. Fernández-Espejo[‡,1], R. Lehembre[†], L. Tshibanda[†,§], A. Vanhaudenhuyse[†], O. Gosseries[†], E. Lommers[†], M. Napolitani[¶], Q. Noirhomme[†], M. Boly[†], M. Papa[‖], A. Owen[#], P. Maquet[†], S. Laureys[†,*] and A. Soddu[†,*]

[†] *Coma Science Group, Cyclotron Research Center, University and University Hospital of Liège, Liège, Belgium*
[‡] *Department of Psychiatry and Clinical Psychobiology, University of Barcelona, Barcelona, Spain*
[§] *Department of Radiology, CHU Sart Tilman Hospital, University of Liège, Liège, Belgium*
[¶] *Department of Clinical Sciences "Luigi Sacco", University of Milan, Milan, Italy*
[‖] *Medicina Pubblica Clinica e Preventiva, Second University of Naples, Naples, Italy*
[#] *MRC Cognition and Brain Sciences Unit, Cambridge, UK*

Abstract: Beside behavioral assessment of patients with disorders of consciousness, neuroimaging modalities may offer objective paraclinical markers important for diagnosis and prognosis. They provide information on the structural location and extent of brain lesions (e.g., morphometric MRI and diffusion tensor imaging (DTI-MRI) assessing structural connectivity) but also their functional impact (e.g., metabolic FDG-PET, hemodynamic fMRI, and EEG measurements obtained in "resting state" conditions). We here illustrate the role of multimodal imaging in severe brain injury, presenting a patient in unresponsive wakefulness syndrome (UWS; i.e., vegetative state, VS) and in a "fluctuating" minimally conscious state (MCS). In both cases, resting state FDG-PET, fMRI, and EEG showed a functionally preserved right hemisphere, while DTI showed underlying differences in structural connectivity highlighting the complementarities of these neuroimaging methods in the study of disorders of consciousness.

*Corresponding authors.
Tel.: +32-4-366-23-16; Fax: +32-4-366-29-46
E-mail: steven.laureys@ulg.ac.be; andrea.soddu@ulg.ac.be

[1]Bruno, M. A and Fernández-Espejo, D equally contributed to the manuscript

DOI: 10.1016/B978-0-444-53839-0.00021-1

Keywords: coma; vegetative state; minimally conscious state; fMRI; EEG; PET; consciousness; traumatic brain injury.

Introduction

The vegetative state (VS) (recently renamed "unresponsive wakefulness syndrome" (UWS)) and minimally conscious state (MCS) are disorders of consciousness (DOC) that can be acute and reversible or chronic and irreversible (Monti et al., 2010). Whereas UWS/VS is characterized by the return of arousal without signs of awareness (The Multi-Society Task Force on PVS, 1994), MCS is defined by the presence of inconsistent but definite behavioral evidence of consciousness of self and/or the environment (e.g., response to command, verbalizations, visual pursuit, etc.; Giacino et al., 2002). An accurate and reliable evaluation of the level and content of consciousness in severely brain-damaged patients is of paramount importance for their appropriate management. Behavioral assessment is one of the main methods used to detect signs of awareness in severely brain injured patients (Majerus et al., 2005). However, clinical practice shows how delicate it is to recognize unambiguous signs of conscious perception in these patients, as one have to make inferences based on the patients' motor responsiveness. Indeed, behavioral assessment may be complicated by the presence of fluctuating arousal levels, motor impairment, tracheotomy, aphasia, agnosia, apraxia, or ambiguous and rapidly habituating responses (Gill-Thwaites, 2006), which may explain the high frequency of misdiagnosis (up to 40%) in these patients (Andrews et al., 1996; Childs and Mercer, 1996; Schnakers et al., 2009).

It is hence essential to employ objective paraclinical markers of consciousness in order to compensate for the lack of clinical reliability at the bedside. Integration of multimodal neuroimaging techniques can enable objective assessment of cerebral function in UWS/VS and MCS patients, and can therefore overcome some of the difficulties in producing an evidence base for predicting their outcome and for their treatment. Resting state [^{18}F]-fluorodeoxyglucose positron emission tomography (FDG-PET), functional magnetic resonance imaging (fMRI), and high-density electroencephalography (EEG) acquisitions are easy to perform and could have a potentially broader and faster translation into clinical practice. The clinical interest of resting state studies is that it allows the investigation of higher order cognitive networks, without requiring patients' active participation, particularly important in DOC. Combining resting state FDG-PET and fMRI studies with structural diffusion tensor imaging (DTI-MRI) analysis can disentangle if the observed functional abnormalities are mostly due to axonal or cortical damages.

In this chapter, we will present two traumatic DOC patients who went through a full battery of behavioral tests combined with multimodal imaging including FDG-PET, resting state fMRI, spontaneous EEG, and DTI measurements.

Data acquisition and analysis

The studies were approved by the Ethics Committee of the Faculty of Medicine of the University of Liege and written informed consent was obtained from all healthy controls and the patients' legal representatives.

FDG-PET

Cerebral metabolism was studied by means of FDG-PET after intravenous injection of 5–10 mCi of FDG on a Siemens CTI 951 R16/31 scanner as described elsewhere (Laureys et al., 1999, 2000a). Patients were monitored by two anesthesiologists

throughout the procedure. FDG-PET data were spatially normalized, smoothed (14 mm full width at a half maximum) and analyzed using Statistical Parametric Mapping (SPM8; www.fil.ion.ucl.ac.uk/spm). Patient data were compared to 39 healthy controls (21 women; age range 18–80 years). SPM analysis identified brain regions with decreased and relatively preserved metabolism in patients as compared to control subjects (global normalization was performed by proportional scaling). The resulting set of voxel values for each contrast, constituting a statistical parametric map of the *t*-statistics (SPM{*t*}), was transformed to the unit normal distribution (SPM{Z}) and thresholded at false discovery rate corrected $p < 0.05$ (Genovese et al., 2002). The number of voxels showing relatively preserved metabolism for the clusters belonging to the same hemisphere were summed up and an asymmetry index was calculated as follows: (# voxels right − # voxels left)/(# voxels right + # voxels left).

fMRI

Resting state BOLD data were acquired on a 3 T MRI scanner (Trio Tim, Siemens, Germany) with an echoplanar imaging (EPI) sequence using axial slice orientation (32 slices; voxel size = $3.0 \times 3.0 \times 3.75$ mm^3; matrix size = $64 \times 64 \times 32$; repetition time = 2000 ms, echo time = 30 ms, flip angle = 78°; field of view = 192 mm). A protocol of 300 scans lasting 600 s was performed. A T1-weighted MPRAGE sequence was also acquired for registration with functional data on each subject. fMRI data were preprocessed using the "BrainVoyager" software package (R. Goebel, Brain Innovation, Maastricht, The Netherlands). Preprocessing of functional scans included 3D motion correction, linear trend removal, slice scan time correction and filtering out low frequencies of up to 0.005 Hz. The data were spatially smoothed with a Gaussian filter of full width at half maximum value of 8 mm. Independent component analysis (ICA) (Formisano et al., 2004) was performed with the "BrainVoyager" software package using 30 components (Ylipaavalniemi and Vigario, 2008). A spatial mean was subtracted from all the voxels of the same spatial map (for each time point) and principal component analysis was applied for dimensionality reduction before performing ICA. The default mode component was selected by visual inspection taking into account both spatial and temporal properties (maps shown in Fig. 1 were obtained by regressing in the BOLD activity with the time course of the default mode independent component used as regressor). Subsequent volumes of interest from the default mode clusters were selected as implemented in Brain Voyager and an asymmetry index was calculated as described above taking into account the number of voxels with preserved connectivity in the default mode of each hemisphere.

EEG

Spontaneous EEG and electro-oculogram were recorded by means of a 60 channel EEG amplifier (eXimia EEG unit, Nexstim Ltd, Finland) for 10 min in resting state conditions. The reference electrode was placed on the forehead and EEG signals were acquired at a sampling rate of 1450 Hz. EEG traces were carefully inspected visually and artifacts were manually marked for rejection using Fast (Leclercq et al., 2009) a toolbox implemented as an extension of SPM and tailored to handle long continuous EEG recordings and to manually score the data (http://www.montefiore.ulg.ac.be/~phillips/FAST.html). For each artifact-free epochs we computed the logarithm of the power at each electrode location using multitaper methods (Percival and Walden, 1993). Average power for all artifact-free epochs were then obtained in the delta [0.5–4 Hz], theta [4–8 Hz], alpha [8–12 Hz], beta [12–36 Hz], and gamma [36–44 Hz] frequency bands. Topographic representations were plotted using the EEGLAB topoplot function (http://sccn.ucsd.edu/eeglab/). An asymmetry index was calculated as described above taking into account the power in the delta band for each hemisphere.

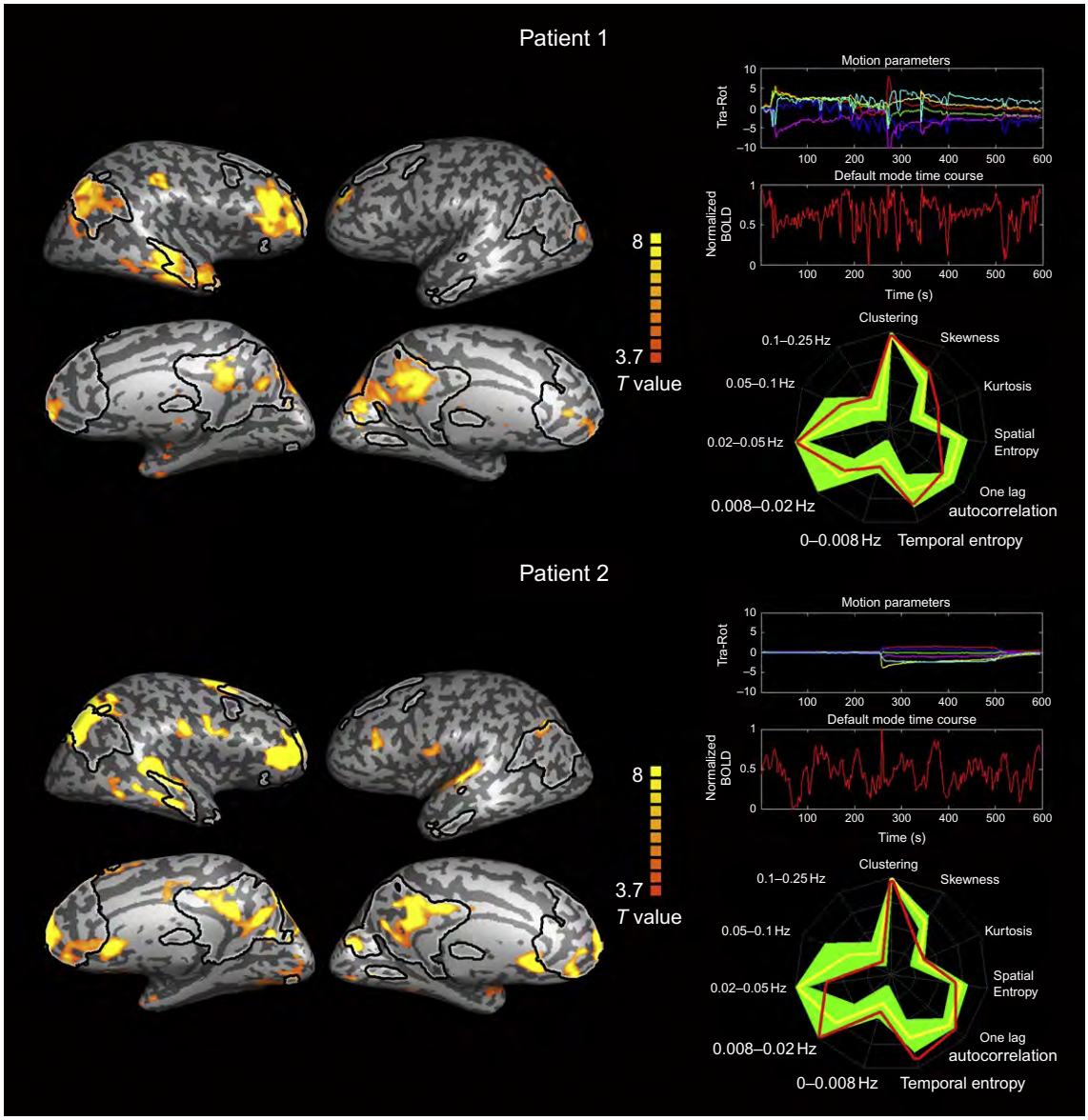

Fig. 1. BOLD resting state default mode connectivity networks in the two patients. Black contour lines indicate the default mode as identified in an independent cohort of 11 healthy subjects. Right panel shows the motion parameters illustrating translation (in mm) for *x* (red), *y* (green), and *z* (blue) and rotation (in °) for pitch (yellow), roll (purple), and yaw (cyan). The default mode time course illustrates the normalized BOLD signal over 600 s. Note the rapid transient "clonic" movement artifacts in the extracted BOLD time series. The fingerprint summarizes the default mode temporal and spatial properties for the patient (red) superimposed to the control data (mean in yellow and standard deviation in green) illustrating that despite the motion artifacts, the extracted network seems of neuronal origin.

DTI

Diffusion-weighted images were acquired using an EPI sequence (TR = 5700 ms, TE = 87 ms, 45 slices; slice thickness = 3 mm, gap = 0.3 mm, matrix size = 128×128) and sensitized in 64 noncollinear directions using a *b*-value = 1000 s/mm^2 and two $b = 0$ images. Raw images were visually inspected for the presence of motion related artifacts. No volumes were discarded as a result of this process. Images were processed using the FMRIB Software Library (FSL; version 4.1.2; http://www.fmrib.ox.ac.uk/fsl). Preprocessing steps included eddy-current correction (Behrens et al., 2003) and skull and non-brain tissue stripping using the brain extraction tool (BET; Smith, 2002). Fractional anisotropy and mean diffusivity maps were obtained using FSL diffusion toolbox (FDT; Behrens et al., 2003). The FMRIB's automated segmentation tool (FAST; Zhang et al., 2001) was used to obtain white matter masks for each patient using fractional anisotropy maps as inputs. After registration, masks were visually inspected and misclassified voxels were removed using FSLView masking tools. Then they were manually split into left hemisphere and right hemisphere masks. An in-house script running on Matlab 7.9 was used to generate histograms from the mean diffusivity maps by allocating the values comprised in the masks to 250 bins, which were normalized by the total number of voxels contributing to the histogram in order to compensate for brain size differences. Whole-brain pathways were traced using DTIquery, a tractography software which uses a streamlines tracking technique to initialize seed points for path tracing at every other voxel in each dimension, evenly sampling the volume with seed points (Sherbondy et al., 2005). We used a step-size of 2 mm, space between seed points of 4 mm, angle of 45°, and a minimum fractional anisotropy of 0.15 to constraint the pathway computation. An asymmetry index was calculated as described above taking into account the peak height of the white matter mean diffusivity histogram of each hemisphere.

Results

Case report 1

A 21-year-old right-handed man suffered from a head trauma during Thai boxing and was admitted to the University Hospital of Liège with a Glasgow Coma Score (GCS) (Teasdale and Jennett, 1974) of 3/15 showing no eye opening, no verbal response, and no motor response to noxious stimulation. Brain CT showed a left subdural hematoma with signs of intracranial hypertension requiring a decompressive craniotomy and drainage of the hematoma. The EEG was characterized by a non-reactive 4–5 Hz basic rhythm with delta dysrythmia more pronounced in the left hemisphere, without paroxistic activity. Structural MRI showed gliotic brainstem lesions with pyramidal tract atrophy and widespread corticosubcortical lesions in the left hemisphere and the corpus callosum and secondary *ex vacuo* hydrocephalus. Tracheotomy and gastrostomy were performed and he was transferred to a rehabilitation center 2 months after the acute brain injury.

After 6 months postinsult, he was transferred to the University Hospital of Liège for standardized behavioral and multimodal neuroimaging assessments encompassing FDG-PET, functional resting state MRI, high-density EEG, and DTI MRI (methodological details are reported below). Coma Recovery Scale-Revised (Giacino et al., 2004) assessment showed a spastic quadriplegia and a tetrapyramidal syndrome, predominantly on the left side, an auditory startle reflex but no response to command, no visual pursuit nor fixation, and stereotyped flexion to pain. Follow-up at 2 year postinjury shows the patient, remaining in a chronic nursing care facility, still in UWS/VS.

Case report 2

A 13-year-old right-handed boy with unremarkable medical history was admitted to the University Hospital of Liège after a traffic accident. On

admission, he showed bilateral areactive mydriasis and GCS assessment showed no eye opening, no verbal response, and no motor response to noxious stimulation (total score 3/15). He was sedated, intubated, and mechanically ventilated. Brain CT-scan showed a left frontotemporoparietal contusion with depressed temporal skull fracture and signs of increased intracranial pressure requiring emergency decompressive craniectomy with ventriculoperitoneal drainage. The EEG showed a nonreactive delta dysrythmia with higher amplitude over the left hemisphere and no paroxistic activity. Structural MRI showed an extradural left frontotemporal hematoma and multiple hemorrhagic lesions in pons, midbrain, corpus callosum, and bilateral frontal and left temporal lobes with secondary hydrocephalus. One month after admission, the patient left the intensive care unit showing spontaneous eye opening and flexion withdrawal to noxious stimulation, fluctuating response to command without communication and bilateral Babinski sign.

Three months postinsult standardized behavioral and multimodal neuroimaging assessments were performed in our unit. Coma Recovery Scale-Revised assessments showed auditory startle reflex without command following or communication, no response to visual threat and no fixation or tracking, flexion to pain and oral reflexive movements. Follow-up at 17 months postinjury learns the patient, remaining in a neurorehabilitation center, is still in a MCS, showing discernible evidence of nonreflex "purposeful" behavior such as visual pursuit, "automatic" motor responses (e.g., grasping the bedrail), and affective behaviors occurring in contingent relation to relevant environmental stimuli.

Multimodal imaging

Resting state FDG-PET data showed for both patients a relatively preserved metabolism (as compared to healthy controls) in the right hemisphere. The left hemisphere showed significant hypometabolic activity for both cases (Fig. 2).

Resting state fMRI showed a right-lateralized preserved default mode network encompassing the precuneal, medial prefrontal, and right temporoparietal cortices in both patients. Note that in both patients the BOLD signal was artifacted by "clonic" motions but the fingerprint analysis showed a "bird shape" suggesting its neural origin (De Martino et al., 2007; Fig. 1).

Resting state high-density EEG showed a left-lateralized high-amplitude delta dysrhythmia (of approximately 1 Hz) in both patients as illustrated in the topographic plots of the delta band (Fig. 3).

DTI tractography showed a marked reduction in the number of identified white matter tracts

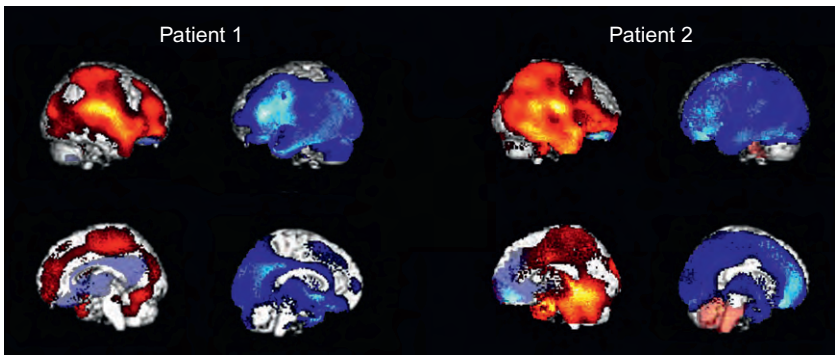

Fig. 2. Statistical parametric mapping analysis identifying brain areas with relatively preserved brain metabolism (in red) and dysfunctional metabolism (in blue) in both patients, as compared to 39 healthy controls. Results are shown on a 3D MRI template and thresholded at false discovery rate corrected $p < 0.05$.

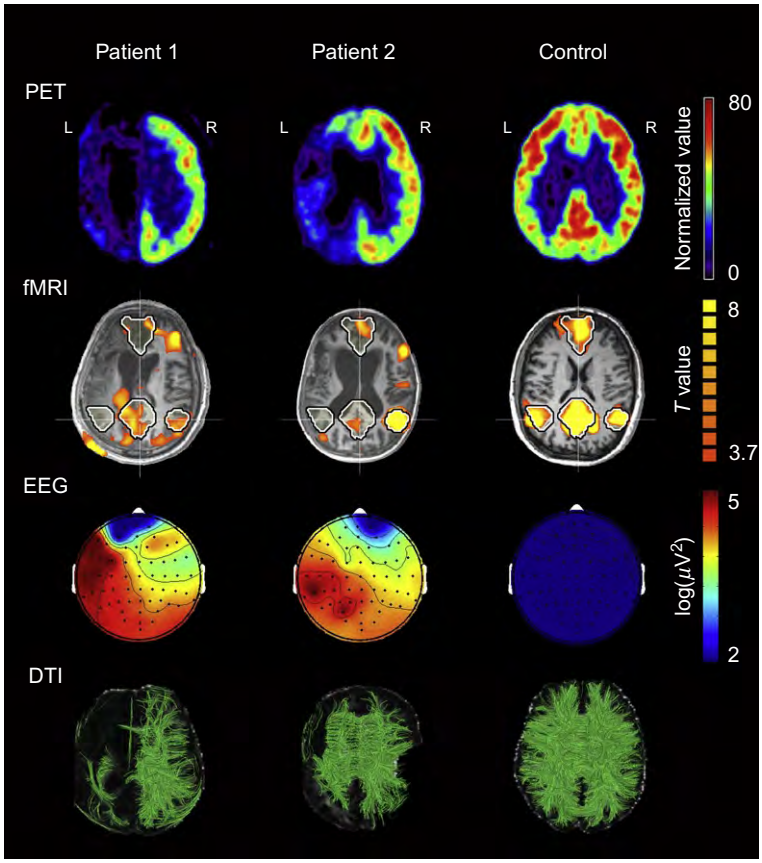

Fig. 3. ^{18}F-fluorodeoxyglucose-Positron emission tomography (FDG-PET), default mode functional MRI, high-density EEG and diffusion tensor imaging (DTI) in two patients with a posttraumatic disorder of consciousness, and an age-matched normal healthy control. PET images show resting state brain metabolism with the color scale ranging from blue (lowest) to red (highest) activity (normalized values). fMRI BOLD resting state connectivity maps overlapping with the normal default mode as extracted from an independent cohort of healthy subjects (black and white contours; colors indicate *T* values). EEG topography maps of averaged power spectra densities in the delta band. Overall delta activity is higher for patients than for controls (colors scale is in $\log(\mu V^2)$). Whole-brain DTI tractography illustrating white matter fiber tracts. Note that both patients show a left hemisphere dysfunction in metabolism and default mode connectivity with lateralized delta dysrhythmia. DTI illustrates that this left-sided "functional hemispherectomy" can have an underlying axonal (patient 1) or cortical (patient 2) pathology.

in the left hemisphere for patient 1 and a much more symmetrical image for patient 2 as confirmed by the DTI asymmetry indexes. Note that FDG-PET and fMRI default mode network connectivity showed a highly asymmetrical pattern in both patients (Table 1).

Discussion

A common pattern of significantly impaired metabolism and resting state fMRI default mode connectivity was observed in our two DOC patients. Previous studies using PET in UWS/VS

Table 1. For each modality we present for left and right hemisphere the number of active voxels (PET), the number of connected voxels belonging to the default mode network (fMRI), the power spectrum in the delta band (EEG) and the mean diffusivity peak height (DTI), with the correspondent asymmetry index in percentage

	Patient 1			Patient 2		
	L	R	AI (%)	L	R	AI (%)
FGD-PET	9.7×10^2	9.4×10^5	98	161	47030	99
fMRI	4.2×10^4	3.1×10^5	76	3.9×10^4	1.9×10^5	66
EEG	188	125	−20	218	122	−28
DTI	2.8×10^{-2}	4.6×10^{-2}	24	3.8×10^{-2}	3.9×10^{-2}	1.3

patients of different etiologies and duration showed that the common hallmark was a metabolic dysfunction of a bilateral frontoparietal network (encompassing bilateral prefrontal regions, Broca's area, parietotemporal, and posterior parietal areas and precuneus) (Laureys et al., 2000c). Posterior cingulate and adjacent precuneal cortices were reported to show most impaired metabolism in UWS/VS (Laureys et al., 1999) and seem to differentiate MCS from UWS/VS patients (Laureys et al., 2004). More recently, a study on patients in the chronic stage of traumatic diffuse brain injury confirmed this bilateral frontoparietal hypometabolism and showed that these regions were more dysfunctional in UWS/VS than MCS patients (Nakayama et al., 2006). Moreover, studies demonstrated that conscious awareness seems not exclusively related to the metabolic activity in the frontoparietal network but, as importantly, to the functional connectivity within this network. UWS/VS patients suffer from long-range corticocortical "functional disconnections" (Laureys et al., 1999, 2000b). These results lead to postulate that certain patients remain unconscious not because of a widespread neuronal loss, but due to the impaired activity in some critical brain areas and to an altered functional relationship between them.

Resting state BOLD results showed a right-lateralized preservation of the default mode network connectivity. The functional and cognitive significance of resting state fMRI data remain controversial and caution in driving conclusions has been advised (Ylipaavalniem et al., 2006). The present case reports of "functional hemispherectomy" DOC patients offer a unique opportunity to better understand the neural origin of the BOLD default mode analyses. In both cases, the dysfunctional hemodynamic fMRI resting state connectivity analyses were corroborated by the more direct metabolic FDG-PET studies, supporting their true neuronal origin rather than originating from noise from the scanner, movement, respiratory, or cardiac artifacts.

Resting state fMRI acquisitions using a common EPI sequence are becoming very suitable for clinical purposes and automatized analysis procedures are nowadays available (Vanhaudenhuyse et al., 2010). On the other hand, in order to use fMRI resting state as a diagnostic tool, important efforts are necessary to handle the artifacts on the BOLD measurements induced by rapid transient "clonic" motions as illustrated in both presented cases. Additionally, highly deformed brains as encountered in DOC patients make group-level analyses and comparisons with healthy control data extremely challenging. User-independent automatic analyses are even more challenging in the functionally asymmetric brains as here presented requiring new strategies to assess resting state fMRI. Important progresses have been reached in the study of fMRI spontaneous brain activity, but in order to make this technique a clinical routine with diagnostic and hopefully prognostic power we will need to tackle the problems of spatial normalization and movement correction together with the issue of strongly asymmetric brains in patients with DOC.

In line with metabolic PET and hemodynamic fMRI results showing left-lateralized impairment, the high-density EEG showed a delta dysrhythmia in the left hemisphere. Indeed it is known that cerebral dysfunctions can be characterized

on the EEG by increased slow electrical activity (Brenner, 2005). Similarly, previous studies in DOC have reported differences in the EEG power spectra between patients in MCS, showing higher power in the delta band than patients with severe neurocognitive disorders (Leon-Carrion et al., 2008).

The presented DOC patients with a "functional hemispherectomy" as shown on resting state metabolic PET and hemodynamic fMRI measurements also benefited from structural DTI analyses aiming to disentangle if the observed functional abnormalities were caused by axonal or cortical damages. DTI-MRI enables characterization of the cerebral microstructure through the observation of molecular movement of water in white matter tracts being sensitive to changes that may not be observable with standard MRI sequences (Le Bihan, 2003). In cases of severe traumatic brain injury, it has been shown a reliable approach to identify the degree of severity (Benson et al., 2007; Huisman et al., 2004) as well as to track the changes that accompany recovery (Sidaros et al., 2008). It is only very recently that DTI has been applied to the study of the DOC (Tshibanda et al., 2009, 2010).

It is commonly assumed that functional connectivity also reflects underlying structural anatomy. Nevertheless, studies relating both measures in healthy subjects have suggested that structural connectivity usually leads to functional connectivity but the inverse relation is not straightforward, as functional connectivity is also observed between regions where there is little or no structural connectivity, because of third regions that may act as a functional link (Damoiseaux and Greicius, 2009). In this sense, the functional asymmetry shown by the two patients might be reflecting different pathologic processes, either having an axonal or cortical basis. In patient 1 the observed left-lateralized functional impairment seems to be related to the left-lateralized structural white matter impairment. In contrary, patient 2 showed dissociation between the lateralized functional impairment and the relatively preserved structural DTI imaging results. A comparable pattern of functional impairment in the default network concomitant to a relative preservation of the white matter, has been previously reported for a UWS/VS patient who, afterward, regained consciousness (Fernández-Espejo et al., 2011). Similarly, Newcombe et al. (2010) have shown that DTI-MRI may help to characterize differences in UWS/VS patients of different etiologies and Fernández-Espejo et al. (2010), using a similar approach albeit restricted to mean diffusivity indices from specific regions of interest have demonstrated differences between UWS/VS and MCS patients.

In conclusion, both posttraumatic DOC patients showed a near normal functioning right hemisphere with severely impaired left cortical networks as documented by metabolic FDG-PET, hemodynamic fMRI, and EEG recordings. These exceptional cases of "functional hemispherectomy" permit to better document the neuronal origin of the default mode "resting state" network as identified by fMRI. Next, the presented cases illustrate that resting state fMRI measurements in DOC patients should be confronted to structural DTI recordings permitting to disentangle different patterns of impairment, with and without axonal disconnections. Future studies should aim to clarify whether both types of impairment have different diagnostic and prognostic value. It is important to stress, that in the absence of a throughout understanding of the neural correlates of consciousness, no strong claims can be made in terms of residual phenomenological awareness in patients with a functionally preserved but isolated right hemisphere function. Split-brain research has previously identified different cognitive processing styles for each cerebral hemisphere (Gazzaniga, 2000). In our view, it cannot be excluded that the clinically UWS/VS patient lacking clinical proof of consciousness as assessed at the bedside, may not show some sensory, core (Damasio, 1998), or primary (Edelman, 2004) consciousness given the observed residual right-lateralized hemispheric function on FDG-PET, fMRI, and EEG measurements.

Acknowledgments

S. L. is Senior Research Associate; A. S., M. B., A. V., Q. N. are Post-doctoral Fellows; and M. A. B. and O. G. are Research Fellow at the Fonds de la Recherche Scientifique (FRS). D. F. E. was supported by a fellowship from the Spanish Ministry for Education (AP2006-00862). This research was supported by the Fonds de la Recherche Scientifique (FRS), the European Commission (DISCOS, Mindbridge, DECODER (ICT Programme Project FP7-247919) & COST), the Concerted Research Action (ARC-06/11-340), the McDonnell Foundation, Mind Science Foundation. The text reflects solely the views of its authors. The European Commission is not liable for any use that may be made of the information contained therein.

Abbreviations

DOC	disorders of consciousness
DTI	diffusion tensor imaging
EEG	electroencephalography
FDG-PET	[^{18}F]-fluorodeoxyglucose positron emission tomography
fMRI	functional magnetic resonance imaging
MCS	minimally conscious state
UWS	unresponsive wakefulness syndrome
VS	vegetative state

References

Andrews, K., Murphy, L., Munday, R., & Littlewood, C. (1996). Misdiagnosis of the vegetative state: Retrospective study in a rehabilitation unit. *British Medical Journal*, *313*, 13–16.

Behrens, T. E., Woolrich, M. W., Jenkinson, M., Johansen-Berg, H., Nunes, R. G., Clare, S., et al. (2003). Characterization and propagation of uncertainty in diffusion-weighted MR imaging. *Magnetic Resonance in Medicine*, *50*, 1077–1088.

Benson, R. R., Meda, S. A., Vasudevan, S., Kou, Z., Govindarajan, K. A., Hanks, R. A., et al. (2007). Global white matter analysis of diffusion tensor images is predictive of injury severity in traumatic brain injury. *Journal of Neurotrauma*, *24*, 446–459.

Brenner, R. P. (2005). The interpretation of the EEG in stupor and coma. *The Neurologist*, *11*, 271–284.

Childs, N. L., & Mercer, W. N. (1996). Misdiagnosing the persistent vegetative state. Misdiagnosis certainly occurs [letter; comment]. *British Medical Journal*, *313*, 944.

Damasio, A. R. (1998). Investigating the biology of consciousness. *Philosophical Transactions of the Royal Society of London. Series B, Biological Sciences*, *353*, 1879–1882.

Damoiseaux, J. S., & Greicius, M. D. (2009). Greater than the sum of its parts: A review of studies combining structural connectivity and resting-state functional connectivity. *Brain Structure & Function*, *213*, 525–533.

De Martino, F., Gentile, F., Esposito, F., Balsi, M., Di Salle, F., Goebel, R., et al. (2007). Classification of fMRI independent components using IC-fingerprints and support vector machine classifiers. *Neuroimage*, *34*(1), 177–194.

Edelman, G. M. (2004). *Wider than the sky: The phenomenal gift of consciousness.* New Haven and London: Yale University Press.

Fernández-Espejo, D., Bekinschtein, T., Monti, M. M., Pickard, J. D., Junque, C., Coleman, M. R., et al. (2011). Diffusion weighted imaging distinguishes the vegetative state from the minimally conscious state. *Neuroimage, 54*(1), 103–112.

Fernández-Espejo, D., Junque, C., Cruse, D., Bernabeu, M., Roig-Rovira, T., Fabregas, N., et al. (2010). Combination of diffusion tensor and functional magnetic resonance imaging during recovery from the vegetative state. *BMC Neurology*, *10*, 77.

Formisano, E., Esposito, F., Di Salle, F., & Goebel, R. (2004). Cortex-based independent component analysis of fMRI time series. *Magnetic Resonance Imaging*, *22*, 1493–1504.

Gazzaniga, M. S. (2000). Cerebral specialization and interhemispheric communication: Does the corpus callosum enable the human condition? *Brain*, *123*(Pt 7), 1293–1326.

Genovese, C. R., Lazar, N. A., & Nichols, T. (2002). Thresholding of statistical maps in functional neuroimaging using the false discovery rate. *NeuroImage*, *15*, 870–878.

Giacino, J. T., Ashwal, S., Childs, N., Cranford, R., Jennett, B., Katz, D. I., et al. (2002). The minimally conscious state: Definition and diagnostic criteria. *Neurology*, *58*, 349–353.

Giacino, J. T., Kalmar, K., & Whyte, J. (2004). The JFK Coma Recovery Scale-Revised: Measurement characteristics and diagnostic utility. *Archives of Physical Medicine and Rehabilitation*, *85*, 2020–2029.

Gill-Thwaites, H. (2006). Lotteries, loopholes and luck: Misdiagnosis in the vegetative state patient. *Brain Injury*, *20*, 1321–1328.

Huisman, T. A., Schwamm, L. H., Schaefer, P. W., Koroshetz, W. J., Shetty-Alva, N., Ozsunar, Y., et al. (2004). Diffusion tensor imaging as potential biomarker of white matter injury in diffuse axonal injury. *AJNR. American Journal of Neuroradiology*, *25*, 370–376.

Laureys, S., Faymonville, M. E., Degueldre, C., Fiore, G. D., Damas, P., Lambermont, B., et al. (2000). Auditory processing in the vegetative state. *Brain*, *123*, 1589–1601.

Laureys, S., Faymonville, M. E., Luxen, A., Lamy, M., Franck, G., & Maquet, P. (2000). Restoration of thalamocortical connectivity after recovery from persistent vegetative state. *The Lancet*, *355*, 1790–1791.

Laureys, S., Faymonville, M. E., Moonen, G., Luxen, A., & Maquet, P. (2000). PET scanning and neuronal loss in acute vegetative state. *The Lancet*, *355*, 1825–1826.

Laureys, S., Goldman, S., Phillips, C., Van Bogaert, P., Aerts, J., Luxen, A., et al. (1999). Impaired effective cortical connectivity in vegetative state: Preliminary investigation using PET. *NeuroImage*, *9*, 377–382.

Laureys, S., Owen, A. M., & Schiff, N. D. (2004). Brain function in coma, vegetative state, and related disorders. *Lancet Neurology*, *3*, 537–546.

Le Bihan, D. (2003). Looking into the functional architecture of the brain with diffusion MRI. *Nature Reviews. Neuroscience*, *4*, 469–480.

Leclercq, Y., Maquet, P., Noirhomme, Q., Degueldre, C., Balteau, E., Soddu, A., et al. (2009). *fMRI Artefact rejection and Sleep Scoring Toolbox (FAST). http://www.monte_ore.ulg.ac.be/phillips/FAST.html.*

Leon-Carrion, J., Martin-Rodriguez, J. F., Damas-Lopez, J., Barroso, Y., Martin, J. M., & Dominguez-Morales, M. R. (2008). Brain function in the minimally conscious state: A quantitative neurophysiological study. *Clinical Neurophysiology*, *119*, 1506–1514.

Majerus, S., Gill-Thwaites, H., Andrews, K., & Laureys, S. (2005). Behavioral evaluation of consciousness in severe brain damage. *Progress in Brain Research*, *150*, 397–413.

Monti, M. M., Laureys, S., & Owen, A. M. (2010). The vegetative state. *British Medical Journal*, *341*, c3765.

Nakayama, N., Okumura, A., Shinoda, J., Nakashima, T., & Iwama, T. (2006). Relationship between regional cerebral metabolism and consciousness disturbance in traumatic diffuse brain injury without large focal lesions: An FDG-PET study with statistical parametric mapping analysis. *Journal of Neurology, Neurosurgery, and Psychiatry*, *77*, 856–862.

Newcombe, V. F., Williams, G. B., Scoffings, D., Cross, J., Carpenter, T. A., Pickard, J. D., et al. (2010). Aetiological differences in neuroanatomy of the vegetative state: Insights from diffusion tensor imaging and functional implications. *Journal of Neurology, Neurosurgery, and Psychiatry*, *81*, 552–561.

Percival, D. B., & Walden, A. T. (1993). *Spectral analysis for physical applications:Multitaper and conventional univariate techniques.* Cambridge, UK: Cambridge University Press.

Schnakers, C., Vanhaudenhuyse, A., Giacino, J., Ventura, M., Boly, M., Majerus, S., et al. (2009). Diagnostic accuracy of the vegetative and minimally conscious state: Clinical consensus versus standardized neurobehavioral assessment. *BMC Neurology*, *9*, 35.

Sherbondy, A., Akers, D., Mackenzie, R., Dougherty, R., & Wandell, B. (2005). Exploring connectivity of the brain's white matter with dynamic queries. *IEEE Transactions on Visualization and Computer Graphics*, *11*, 419–430.

Sidaros, A., Engberg, A. W., Sidaros, K., Liptrot, M. G., Herning, M., Petersen, P., et al. (2008). Diffusion tensor imaging during recovery from severe traumatic brain injury and relation to clinical outcome: A longitudinal study. *Brain*, *131*, 559–572.

Smith, S. M. (2002). Fast robust automated brain extraction. *Human Brain Mapping*, *17*, 143–155.

Teasdale, G., & Jennett, B. (1974). Assessment of coma and impaired consciousness. A practical scale. *Lancet*, *2*, 81–84.

The Multi-Society Task Force on Pvs, (1994). Medical aspects of the persistent vegetative state (1). *The New England Journal of Medicine*, *330*, 1499–1508.

Tshibanda, L., Vanhaudenhuyse, A., Boly, M., Soddu, A., Bruno, M. A., Moonen, G., et al. (2010). Neuroimaging after coma. *Neuroradiology*, *52*, 15–24.

Tshibanda, L., Vanhaudenhuyse, A., Galanaud, D., Boly, M., Laureys, S., & Puybasset, L. (2009). Magnetic resonance spectroscopy and diffusion tensor imaging in coma survivors: Promises and pitfalls. *Progress in Brain Research*, *177*, 215–229.

Vanhaudenhuyse, A., Noirhomme, Q., Tshibanda, L. J., Bruno, M. A., Boveroux, P., Schnakers, C., et al. (2010). Default network connectivity reflects the level of consciousness in non-communicative brain-damaged patients. *Brain*, *133*, 161–171.

Ylipaavalniem, J., Mattila, S., Tarkianen, A., & Vigaro, R. (2006). Brains and phantoms: An ICA study of fMRI. Independent component analysis and blind signal separation. In *6th International Conference, Ica 2006, Proceedings,* pp. 503–510. Berlin Heidelberg: Springer-Verlag.

Ylipaavalniemi, J., & Vigario, R. (2008). Analyzing consistency of independent components: An fMRI illustration. *NeuroImage*, *39*, 169–180.

Zhang, Y., Brady, M., & Smith, S. (2001). Segmentation of brain MR images through a hidden Markov random field model and the expectation-maximization algorithm. *IEEE Transactions on Medical Imaging*, *20*, 45–57.